Effective-charge theory for the electronic stopping of heavy ions in solids: Stripping criteria and target-electron models

Richard J. Mathar and Matthias Posselt
Institut für Ionenstrahlphysik und Materialforschung, Forschungszentrum Rossendorf e.V., Postfach 510119, 01314 Dresden, Germany
(Received 13 June 1994)

The calculation of the ionization fraction of the ion as a function of the ion atomic number, ion velocity and target Fermi velocity is the first step in effective-charge theory for heavy-ion stopping. We show results using the energy stripping criterion for the ionization fraction and give reasons for its superiority as against the velocity stripping criterion. The second computational step is the transformation of the ionization fraction into an effective-charge fraction assuming a linear dynamic dielectric response of the target material. On the basis of the Kaneko shell theory of solid targets we explain, to what extent the simple free-electron gas model still may work, if the heavy-ion stopping calculation makes use of the heavy-ion scaling rule and experimental proton stopping data.

I. OVERVIEW

The effective-charge theory for heavy-ion stopping in solids is a particular form of the dielectric theory of the electronic part of ion stopping that describes the energy loss by the electrodynamic force of the charges induced in the target onto the ion. As an extension of the Lindhard-Winther theory[1] of pointlike charges, the fundamental model was given by Brandt and Kitagawa[2] (BK) and became the basis of the calculation of the heavy-ion electronic stopping by Ziegler, Biersack, and Littmark (ZBL).[3] Selected aspects of these works are reviewed in Sec. II. Though the determination of the ionization fraction of the ion is the first central step of effective-charge theory, its theoretical understanding is rather limited. Section III argues for the energy criterion to explain the stripping degree of the ion as a function of ion velocity, ion atomic number, and target Fermi velocity v_F. This work is motivated by the preference given by BK and ZBL to the competing velocity criterion.

The second step calculates the charges induced in the target, taking its dynamic dielectric response from a free-electron gas with the experimental Fermi energy, and their stopping (Coulomb) force back onto the ion. It makes clear why the ion with charge Qe is "effectively" stopped more than a point charge Qe and less than a bare ion nucleus Z_1e. Q denotes the ion charge number, e the elementary charge unit, Z_1 the ion atomic number, and $q \equiv Q/Z_1$ the ionization fraction. Within linear response the heavy-ion stopping cross section $S(q, v, Z_1)$ is less than Z_1^2 times the stopping of a proton at the same velocity v, where hydrogen is assumed to be fully stripped. A useful description of this deviation is the definition of the effective-charge fraction γ,

$$S(q, v, Z_1) \equiv (\gamma Z_1)^2 \, S(q = 1, v, Z_1 = 1) \qquad (1)$$
$$(q < \gamma < 1).$$

On the one hand γ is predicted by effective-charge theory; on the other hand it is available from the ratio of experimental heavy-ion and proton stopping data. Instead of using the heavy-ion stopping calculated in the second step, ZBL enter into a third computational step. Only the theoretical effective-charge fraction γ is retained. The final heavy-ion stopping at the left-hand side (lhs) of (1) is computed inserting the experimental proton stopping into the rhs, now using it as the "heavy-ion scaling rule." The experimental proton data introduce and add the indispensable contribution of the target core electrons to the stopping. Section IV deals with the related question, why can the target dielectric function modeled by a homogeneous electron gas still be sufficient to calculate γ, though it represents only the polarization of the top valence band and conduction electrons? We want to give an answer from the viewpoint of an extended description of the target electrons. The aim beyond that is to let the third heuristic scaling step become superfluous. Instead, the heavy-ion stopping should be determined directly in a modified second step on the basis of a more realistic target-electron model.

II. BRANDT-KITAGAWA THEORY AND ZBL MODIFICATIONS

The BK theory[2] describes an ion with $N = Z_1 - Q$ bound electrons by the radial symmetric particle density

$$\rho_e(r) = N \exp(-r/\Lambda)/(4\pi\Lambda^2 r) \qquad (2)$$

(Λ is the ion size parameter). The total energy of the electrons is built by the sum of the local density approximation (LDA) of the kinetic energy, the Hartree approximation to the electron-electron interaction, and the Coulomb energy of the electrons in the field of the nuclear charge. A variational coupling factor λ was introduced to correct for missing exchange and correlation terms. With ρ_e from above, the total energy of the bound electrons reads

$$E_{\mathrm{BK}} \equiv \frac{\hbar^2}{m} a \frac{N^{5/3}}{\Lambda^2} + \lambda \frac{e^2}{4\pi\epsilon_0} \frac{N^2}{4\Lambda} - \frac{e^2}{4\pi\epsilon_0} \frac{Z_1 N}{\Lambda} \qquad (3)$$

($a \equiv 0.24005$, m is the electron mass, $\hbar$ is the reduced Planck's constant, SI units throughout). The size parameter Λ was determined to minimize this energy,

$$\Lambda \equiv 2a(1-q)^{2/3} a_0 / \left[Z_1^{1/3} \{1 - \lambda(1-q)/4\} \right] \qquad (4)$$

(a_0 is the Bohr radius). We note that factors in corresponding expressions in Refs. 3–5 were erroneous. The same Λ is obtained by applying the virial theorem to the three terms of E_{BK}. λ had to be 4/7 to let the neutral atom of an element have lower energy than its ions. The binding energy E_{BK} is close to the Thomas-Fermi (TF) model.[6] Both lie approximately 20% below the more accurate Hartree-Fock energies of the Clementi-Roetti (CR) tables[7] (Fig. 1). The overestimation of the binding energies of the electrons in the nuclear field arises from the singularities of the charge densities at $r = 0$ in both models.

The electronic stopping cross section S per target electron was obtained from the generalized Lindhard-Winther theory of the stopping in a homogeneous electron gas with electron density n and Lindhard dielectric function ϵ:[8]

$$S = \frac{Z_1^2 e^4}{4\pi\epsilon_0^2 m v^2} L, \qquad (5)$$

$$L \equiv \frac{i\epsilon_0 m}{\pi e^2 n} \int_0^\infty \frac{dk}{k} \left| \frac{\rho_m(k)}{Z_1} \right|^2 \int_{-kv}^{kv} \omega \left[\frac{1}{\epsilon(k,\omega)} \right] d\omega \qquad (6)$$

(L is the stopping number, k is the wave number). The form factor $\rho_m(k)$ is the Fourier transform of the total charge number density, the nuclear part $Z_1\delta(r)$ plus $\rho_e(r)$. In the BK theory, Eq. (2) yields

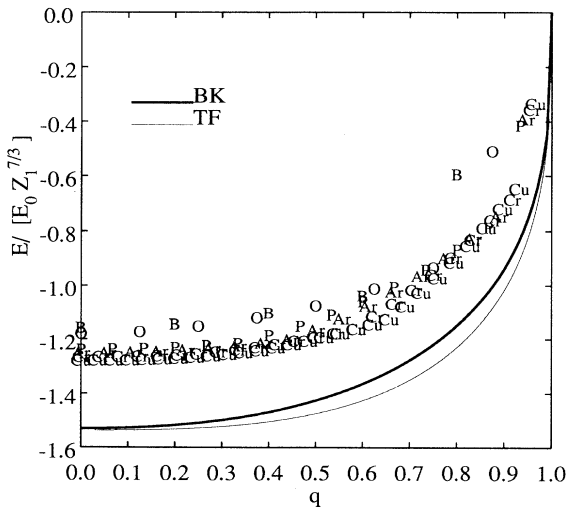

FIG. 1. Scaled ion energies. Thick line: BK energy, Eqs. (3) and (4). Chemical symbols: CR (Ref. 7) energies. Thin line: TF energy ($E_0 = 1$ Ry ≈ 13.6 eV).

$$\rho_m(k) \equiv \rho_n(k) + \rho_e(k) = Z_1 - N/\left[1 + (k\Lambda)^2\right]. \qquad (7)$$

For small momentum transfer $\hbar k$, which means soft, distant collisions, $\rho_m(k)$ approaches Q — the ion looks like a charge Qe to the target electrons. At large k, which means hard, close collisions, $\rho_m(k)$ approaches Z_1 and they feel more of the nuclear charge. The unrealistic model charge density nearby the ion nucleus influences only the high-k limit of ρ_m. There it is suppressed by the multiplication with the energy loss function $\propto 1/\epsilon$, if the target Fermi velocity v_F and wave number k_F are chosen realistically: The imaginary part of $1/\epsilon$ is zero for the Lindhard dielectric function if $k > 2k_F(v/v_F + 1)$. The target electrons cannot resolve the inner ion structure. Therefore the stopping power calculation suffers less from this weakness of the ion model than the total electron binding energy.

Given some ionization fraction q, the theory predicts the stopping cross sections of heavy ions and protons by (5) and (6) and the effective-charge fraction γ by (1) out of their ratio at equal velocity.

In Secs. III A and IV C we shall deduce ionization fractions from effective-charge fractions. The effective-charge fractions of ZBL (Refs. 3 and 9) will be taken as a reliable starting point, rather than the results of the BK theory, because of the larger amount of experimental data. The following brief discussion enlightens the consequences of the ZBL modifications of the "inner" variables in the BK theory.

ZBL simplified a formula for γ, already given by BK as a good approximation in the region $S \propto v$:

$$\gamma = q + \tfrac{1}{2}(1-q)\,(v_0/v_F)^2 \ln\left[1 + (4\tilde{\Lambda}k_F/1.919)^2\right] \qquad (8)$$

(v_0 is the Bohr velocity). The ion size parameter $\tilde{\Lambda}$ was generally increased compared with expression (4), and multiplied with a tabulated factor individual to Z_1 [Fig. 2(a)]. At low velocities, when q is small and the term $\propto 1 - q$ dominates the rhs of (8), this modification creates the Z_1 oscillations of Fig. 3, which are missing in the BK ion model. ZBL told that the plateaus in $\tilde{\Lambda}(q)$ account for the enhanced K-shell screening, but they are not really correlated with the number of bound electrons.

Using (8), an increase of the target-electron density slightly reduces γ at constant ion parameters and low velocities: $\partial\gamma(q,\tilde{\Lambda},v_F)/\partial v_F < 0$, opposite to the BK results. Therefore, (8) contradicts the comprehension that an increase of v_F places more target electrons near to the ion nucleus and should increase γ.[2] This unique sign of this partial derivative is not found in Fig. 3, however, but the curves of Mg targets cross the curves of Si targets of the same velocity. The reasons are that (i) the ion parameter q is not a constant in the ZBL description, but depends on Z_1 itself, and (ii) in fact (8) is only used exactly, if the velocity is high enough to let $\tilde{v}_r > \max(v_0, 0.13 Z_1^{1/3} v_0)$ hold (see below). It should be kept in mind that (8) was intended to deliver stopping numbers in conjunction with an universal fit of the ionization fraction q, but neither fit was claimed to hold on its own.

The ionization fraction was derived from experimen-

tal data as a fit function of the effective ion velocity $y_r \equiv v_r/(v_0 Z_1^{2/3})$, assuming the validity of (8). The resultant ZBL ionization fraction is given in Fig. 4. The choice of y_r as the scaling variable was motivated by the velocity stripping criterion (Sec. III B). The velocity variable depends on the target Fermi velocity via

$$\tilde{v}_r \equiv \begin{cases} v\left[1+\frac{1}{5}(\frac{v_F}{v})^2\right] & \text{if } v \geq v_F, \\ \frac{3}{4}v_F\left[1+\frac{2}{3}(\frac{v}{v_F})^2-\frac{1}{15}(\frac{v}{v_F})^4\right] & \text{if } v \leq v_F, \end{cases} \tag{9}$$

as proposed by Mann and Brandt,[4,10] but additional limits were set in the ZBL program:

$$v_r \equiv \max\{v_0, \tilde{v}_r, 0.13 v_0 Z_1^{2/3}\}. \tag{10}$$

Unfortunately the ZBL redefinition of the ion size parameter Λ did not need to account for a reliable conservation of the electron binding energy, because the energy does not come into play during our second calculational step, the calculation of effective-charge fractions. If, for example, $\tilde{\Lambda}$ is inserted into the BK energy functional (3), the binding energies look like in Fig. 2(b) and, e.g., show an energy minimum for $_{18}Ar^{5+}$ instead of $_{18}Ar^0$. It is not even clear whether the ZBL fit of ion parameters implies some different form of the energy functional. Since the energy of the "ZBL ion" is neither known nor defined, the direct comparison of energy criterion predictions (Sec. III C) with the ZBL ionization fraction is impossible. Therefore, in Sec. III A we switch to ion models with available electron binding energies.

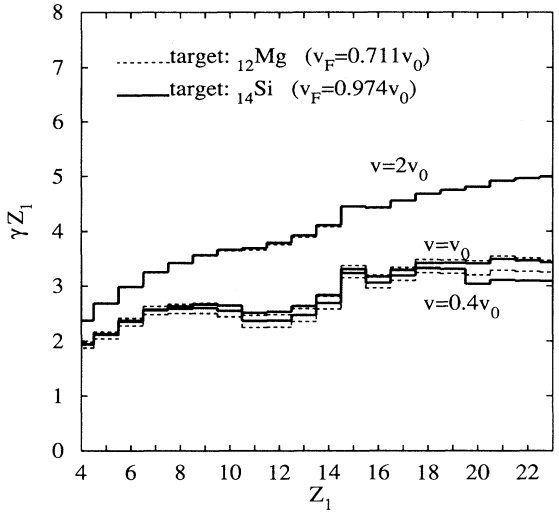

FIG. 3. Effective charges γZ_1 by the ZBL program for ion velocities $0.4v_0$, v_0, and $2v_0$ and targets $_{12}$Mg and $_{14}$Si.

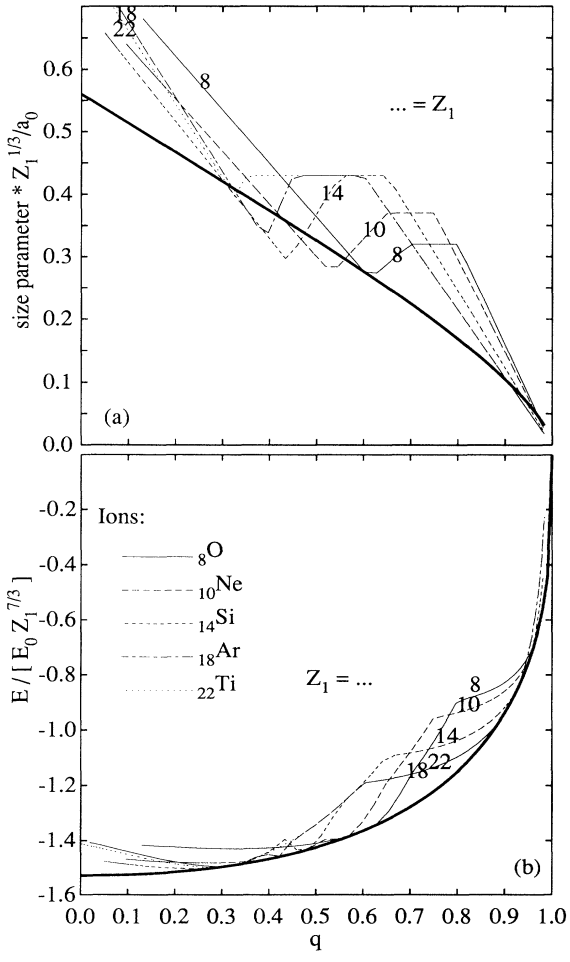

FIG. 2. (a) Ion size parameters. (b) Ion energies if the size parameters of (a) are inserted into (3). The smooth thick lines denote the BK ion model with size parameter Λ, the thin lines examples from the ZBL parameter $\tilde{\Lambda}$ (practically independent of targets).

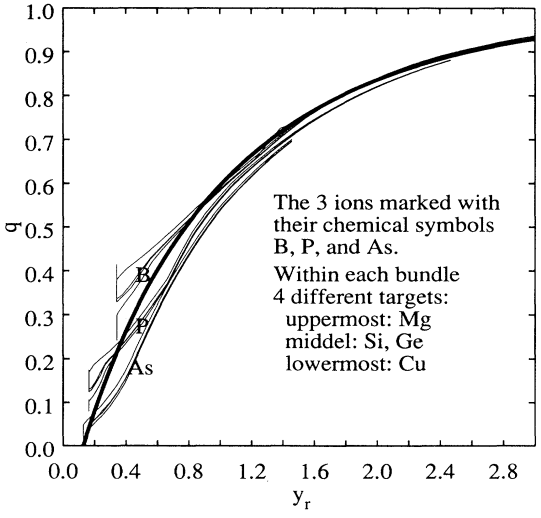

FIG. 4. Thick line: ZBL ionization fraction q vs effective ion velocity y_r. Thin lines: ionization fractions with ZBL effective charge fractions γ but fully integrated BK ion and Lindhard dielectric function. Vertical lines comprise results from different velocities v that are mapped onto a common y_r by (10).

III. ENERGY AND VELOCITY STRIPPING CRITERIA

A. Deducing ionization fractions: Ion models

Ionization fractions deduced from experimental effective-charge fractions greatly depend on the ion model and treatment of the stopping number integral in (6). The hidden values of q are estimated from measured γ by transformation formulas like (8).

To give an idea of the differences that emerge from diverse handlings of these transformations, Fig. 4 shows ionization fractions that reproduce the effective-charge fractions of ZBL, but result from the calculation of the electronic stopping cross sections of protons and heavy ions by numerical integration of the BK ion form factor (7) and the Lindhard energy loss function. Two effects contribute to the changes compared with the ZBL ionization fraction. (i) The low-velocity ZBL approximation (8) always underestimates γ compared with the fully integrated stopping number and generally compensates it by assuming a larger q. (ii) At low velocities, γ is additionally increased by the increased ion size parameter $\tilde{\Lambda}$ [cf. Fig. 2(a)], which demands a lower q for compensation.

A more precise ion model is given by the ion charge distributions tabulated by Clementi and Roetti, based on the Hartree-Fock method.[7]

Figure 5 compares CR with BK electronic stopping powers from the fully integrated (6) at fixed ionization fractions. The CR free ion charge densities generate higher stopping powers at small q. The centers of the outer CR ion shells with wave functions $\propto r^{n-1}e^{-\zeta r}$ are more distant from the nucleus than the tighter BK charges, let pass more target electrons through less shielded ion regions, and increase the stopping. Though the CR charge densities and energies (cf. Fig. 1) show definite shell effects, we see no equivalent bunching of the stopping curves of equal principal quantum number, because the target one-electron radius is larger than the inner ion shell radius. This resolution argument has been given in Sec. II in momentum space. The difference between the CR and BK electronic stopping thus vanishes at large Q.

Deducing q from a given effective-charge fraction is restricted to the finite set of integer Q values in the case of CR ions. The calculated q values, however, stay below the estimates of the BK ion model (Fig. 4) as a consequence of the different stopping powers, and even below the ZBL curve at low velocities.

Figure 6 results from a check on the presence of Z_1 oscillations of CR ions. The effective-charge γZ_1 does not show the distinct minimum at $Z_1 = 10, \ldots, 12$, predicted by scattering theory and density functional calculations,[11–13] but only a weak reduction. Two other characteristic features of the Z_1 oscillations are reproduced. (i) If v is above the limit for plasmon excitation, the structures diminish, and (ii) at lower v_F they are more pronounced. The effective-charge treatment cannot explain Z_1 oscillations by the filling of open ion shells, mediated by Friedel's sum rule. The essential prerequisite is absent: Charges induced in the free-electron target are calculated with incomplete regard to the ion charge. ϵ does not comprise a self-consistent electron excitation spectrum and not the phase space blocking imposed by the electrons bound to the ion.[14] The mutual interaction between the ion charge and induced charges is merely described within the Hartree approximation. The structures obtained here result from their spatial overlap.

B. Velocity criterion

The velocity criterion to explain the dependence of the ionization fraction q on the ion velocity reads as follows: Electrons are stripped, if their orbital velocity v_e is less than the ion velocity v.[2,15–17] The BK theory added a fit parameter b, named stripping parameter,

$$bv_e(r_q) = v,$$

and modeled the ion by a neutral TF atom with the electrons outside the cut radius r_q stripped:

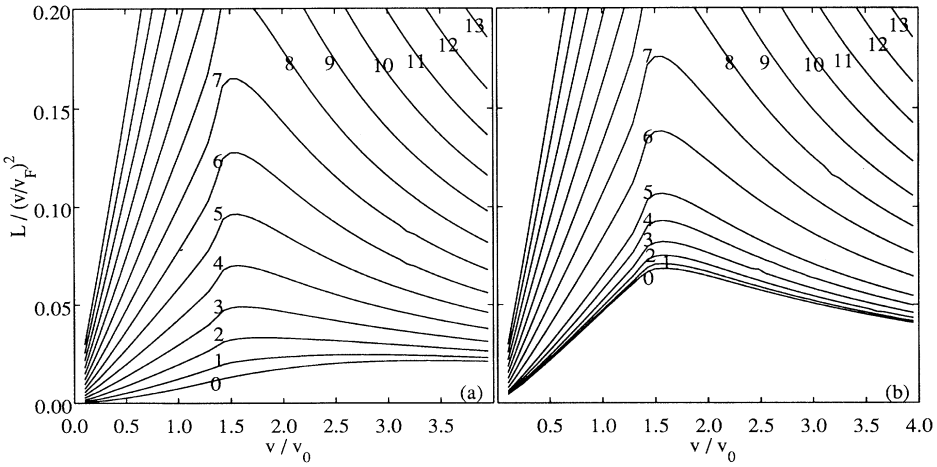

FIG. 5. Energy losses $L/(v/v_F)^2$ by (5) with projectile $_{15}$P, the Lindhard dielectric function inserted into ϵ and $v_F = v_0$. Numbers at curves denote the ion charge numbers Q. (a) BK ion model. (b) CR charge densities.

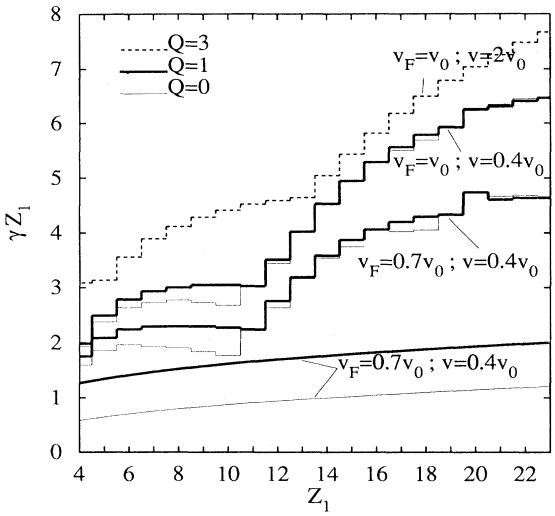

FIG. 6. Effective charges γZ_1 of atoms (charge number 0) and ions (charge numbers 1 and 3) by (5), using the fully integrated Lindhard dielectric function for protons and projectiles. The five stepped upper curves result from inserting CR ions into ρ_m, whereas the two smooth lower stem from the BK ion model, (7). Plasmons are excited at $v > 1.36v_0$ if $v_F = v_0$, at $v > 0.986v_0$ if $v_F = 0.7v_0$.

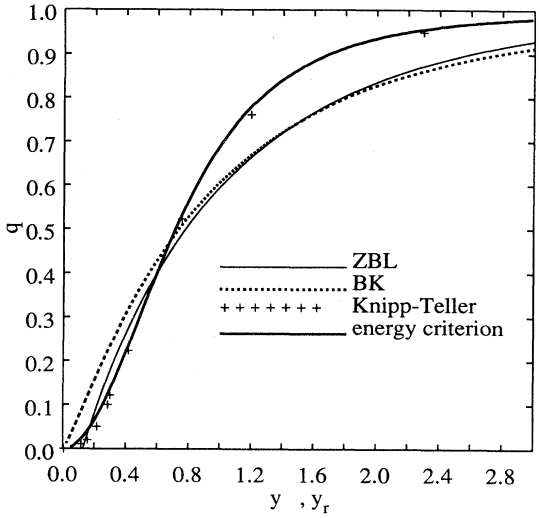

FIG. 7. Thick line: ionization fraction from energy criterion with total energy $E_{\rm BK} + \frac{1}{2}mv^2N$, Eq. (14). Crosses: values by Knipp and Teller (Ref. 20). Thin solid line: ZBL ionization fraction. Dotted thin line: BK ionization fraction, Eq. (11).

$$Q = \int_{r>r_q} \rho(r) d^3r.$$

$\rho(r)$ represents the electron density of the neutral TF atom. It was linked to the orbital velocity $v_e(r)$ via the LDA. In terms of the standard reduced variables Φ and x of the TF equation[6] the BK ionization fraction $q(v)$ is reproduced by the implicit representation

$$\frac{v}{v_0 Z_1^{2/3}} = b\sqrt[3]{\frac{32}{3\pi}}\sqrt{\frac{\Phi}{x}} \quad \text{and} \quad q = \Phi - x\frac{d\Phi}{dx}, \tag{11}$$

where $\Phi(x)$ is the solution of the TF equation of the neutral atom. This ionization fraction is shown in Fig. 7 as a function of the variable $y \equiv v/(v_0 Z_1^{2/3})$. The adjustable stripping parameter b was found to be 1.33 for best agreement with experiments.

C. Energy criterion

The energy stripping criterion to explain the dependence of the ionization fraction on the ion velocity was formulated as follows: The total energy E of the N bound electrons in the target frame of reference is minimized.[15,18] For ion models with integer N or for statistical ion models this means alternatively

$$\min\{N\} : E(N-1) \geq E(N) \quad \text{or} \quad \frac{\partial E(N, v, Z_1, \ldots)}{\partial N} = 0. \tag{12}$$

The second form is the lowest-order Taylor approximation to the first. The total energy E generally comprises the potential and kinetic energies of the bound electrons. It may be split into the inner ion energy E_i, measured in the ion frame of reference, and the center-of-mass part of the total kinetic energy, measured in the target frame of reference:

$$E = E_i + \frac{1}{2}mv^2N. \tag{13}$$

The energy criterion tests for each N whether the gain of kinetic energy of an electron that has been stripped and has come to rest in the target suffices to procure the increase of the inner energy. The energy ansatz requires a good separation of two time scales: The ion state must change slowly compared with the collision time with the target electrons. Rather independent of the ion atomic number and velocity, ions change their charge state by one elementary charge unit within 100–200 fs, whereas the collision time is about three orders of magnitudes smaller. This close contact of the ion with the target-electron "bath" ensures that the inner variable q follows changes of v with practically no delay and we may relate $E_i(q)$ with the kinetic energy at velocity v.

A basic realization is obtained from the BK ion energy, E_i equal to $E_{\rm BK}$ as defined by Eqs. (3) and (4). Insertion of E into (12) yields

$$6a(1-q)^{2/3}y^2 \equiv \left[1 - \frac{\lambda}{4}(1-q)\right]\left[1 - \frac{7}{4}\lambda(1-q)\right], \tag{14}$$

plotted in Fig. 7. Some arguments[3] that were given to support the superiority of the velocity criterion do not hold:

(a) As the mean kinetic energy per bound electron in the TF or BK ion model is proportional to $Z_1^{4/3}$, the

velocity criterion yields a universal scaling parameter $y \propto v/Z_1^{2/3}$. The same scaling results from the energy criterion applied to ion models with energies of the form $E_i \propto Z_1^{7/3} f(q)$ as well. Equation (14) proves it for the BK ion.

(b) In the limit of effective one-electron potentials $\propto 1/r$, the virial theorem unifies both criteria.[15] The work of Northcliffe[19] deals with ions stripped up to the K shell, where this limit is realized. Therefore it cannot be quoted to decide which criterion agrees better with experiments.

(c) Knipp and Teller[20] calculated ionization fractions of the TF ion close to our results of the energy criterion on the BK ion by looking at "electronic velocities within the ion" (cf. Fig. 7). Their formula is obtained from the energy criterion starting with $dE/dN = (dE/d\mu)/(dN/d\mu)$, where μ denotes the TF chemical potential. Their wording "mean square velocity" actually means the kinetic and binding energies and is misleading in our classification.

On the other hand, the correctness of the energy criterion is made clear by the following items:

(i) The energy criterion predicts that q is not proportional to y at small y, contrary to the velocity criterion (Fig. 7). Instead, the low-velocity approximation of (14) is $q \approx 7ay^2$, and the resultant "knee" fits better with the ZBL gap on the y axis at low energies. This power law reflects the first ionization energy of the BK ion, which is proportional to $Z_1^{1/3}$ and set equal to $\frac{1}{2}mv^2$ by the energy criterion.

(ii) The energy criterion is open to improvements concerning the quantum mechanical treatment of the ion energies — without an equivalent for the velocity criterion. For example, Fig. 8 gives the plateaus of stability of an integer number of bound electrons by the discrete version and the CR ion energies. The gaps on the y axis are the analog of the delayed rise of $q(y)$ in (i) in the case of ion models with nonzero first ionization energies and the discrete version of the criterion. The steep parts arise from the comparable magnitudes of successive ionization energies of open K or M shells.

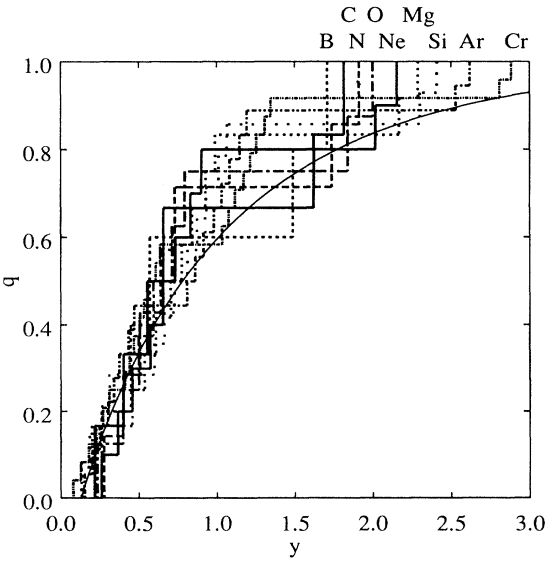

FIG. 8. Thick lines: ionization fractions by the discrete version of the energy criterion with $E = E_{\mathrm{CR}} + \frac{1}{2}mv^2N$ [E_{CR} is the Clementi-Roetti (Ref. 7) ion energy]. Thin smooth line: ZBL ionization fraction.

(iii) ZBL demonstrated an improved universal scaling $q(y)$, if the ion velocity v is replaced by a relative velocity v_r, Eq. (9). The energy criterion implies this improvement, too. The c.m. kinetic energy of the bound electrons was written $\frac{1}{2}mv^2N$ in the target frame of reference. Actually, the maximum total energy available to the stripping process must be calculated from the total kinetic energy in the c.m. system of the colliding partners. The velocity of the colliding target electrons defines a statistical frame of reference with velocity differences between $v - v_F$ and $v + v_F$. The mean of the squared velocity is increased just as calculated by ZBL. The thermodynamic point of view describes this term by the replacement $E_{\mathrm{BK}} \to E_{\mathrm{BK}} + \mu N$, where μ is the Fermi energy of the host material. This shifts the minimum of E_{BK} with respect to N from $q = 0$ to $q \approx 7a\mu/(E_0 Z_1^{4/3})$ and predicts an energy increase of about μZ_1, which is, up to shell effects, in accordance with results from density functional calculations.[21]

(iv) The BK ionization fractions, which were calculated from the velocity criterion, are closer to the ZBL values than those from the energy criterion (cf. Fig. 7). But this gives no reason to claim the superiority of the velocity criterion, since it was only achieved by the installation and adjustment of the stripping parameter b. The following criticism of the energy criterion in the simple form (12) gives the physical understanding, why a corresponding substitution of $mv^2N/2$ by $mv^2N/(2b^2)$ must be introduced on its part in (13). The excess energy $\frac{1}{2}mv^2$ per bound electron compares virtual steady-state situations with more or fewer electrons stripped, with no regard to the physical transition process. The energy criterion must be reinterpreted as a comparison of the ionization energies with the energies actually transferable during capture or loss processes. Target electrons lose their kinetic energy by excitation of the bound electrons under the kinematical restrictions of momentum and energy conservation. This partitioning of the energy with later radiative or nonradiative deexcitation may effectively catch electrons though their energy $\frac{1}{2}mv^2$ exceeds the suitable energies of free ion orbitals. The same mechanisms reduce the available energy transferred from a target electron to a bound electron, which is a candidate for being stripped.

In a simple mechanical model the target electron may collide with a subset of $\tilde{N}$ of the bound electrons, and the rest of them are treated as spectators, an external potential. Under the constraint of energy and momentum conservation the resultant stripping parameter is $(1 + 1/\tilde{N})^{1/2}$, thus interpolating between 1 (low velocities, $\tilde{N}$ large) and 1.41 (high velocities, $\tilde{N} = 1$). The best fit to the experimental $q(y_r)$ is the identification of $\tilde{N}$ with the number of electrons still bound in the outer shell. Applied to Fig. 8, this concept flattens the steep parts

with open K and M shells, since the high-q endings with nearly empty shells and small $\tilde{N}$ are transferred more into the high-v direction than the low-q endings. Summing up, the reciprocal of the stripping parameter is a degree of efficiency of the energy transfer between target and bound electrons.

IV. TARGET DESCRIPTION: FREE-ELECTRON GAS, SHELLS

A. Kaneko theory

The Kaneko theory[22] calculates the total electronic stopping cross section of one target atom by the sum of cross sections of free electrons and shells of bound electrons,

$$S = \sum_{\text{free,bnd}} N_{\text{shell}} S_{\text{shell}}$$

(N_{shell} is the number of electrons per atom in the shell). The free-electron cross sections are taken from the Lindhard theory; some elemental targets are exclusively composed of bound electron parts ($N_{\text{free}} = 0$). The momentum expectation values of electrons in bound shells are fitted by Gaussian distributions with characteristic wave numbers $\bar{q}$. The equivalent characteristic velocities and density parameters are $\bar{v} \equiv \hbar\bar{q}/m$ and $\chi^2 \equiv 1/(\pi\bar{q}a_0)$. The dielectric functions $\epsilon(k,\omega)$ are calculated within the random phase approximation (RPA) independently shell by shell by insertion of the Gaussian occupation probabilities in momentum space. In local space, the ground state density continues to be homogeneous for both free and bound electrons. A local variant, derived from a superimposed local plasma approximation, was applied by Xia *et al.* to the low-velocity heavy-ion stopping.[12,23] Following the linear dielectric response treatment of Lindhard and Winther,[1] the stopping cross sections of bound target electrons are

$$S_{\text{bnd}} = \frac{Z_1^2 e^4}{4\pi\epsilon_0^2 m v^2} L_{\text{bnd}},$$

$$L_{\text{bnd}} \equiv -\frac{8}{\pi^{3/2}\chi^2}\int_0^\infty z\left|\frac{\rho_m(z)}{Z_1}\right|^2 dz \int_0^{v/\bar{v}} u\,\text{Im}\frac{1}{\epsilon(z,u)}du,$$

with $z \equiv k/(2\bar{q})$ and $u \equiv \omega/(\bar{v}k)$ here.

The Kaneko model predicts rather accurate proton stoppings. They are slightly above the ZBL values at $v \gtrsim 4v_0$, and slightly below in the region of $S \propto v$. The latter is a feature well known from the RPA of the dielectric function of the free-electron gas. The free electrons supply the major part of the proton stopping at low velocities; therefore the total cross section is underestimated, too. The former, to our belief, is caused to some extent by an overestimation of the phase space available to excited target electrons. The present model and dielectric functions permit the electron excitation by an arbitrary energy transfer $\hbar\omega$ for any shell, which is justified for the free-electron parts but not for the bound electrons. We have tested the influence of a simple correction for the excitation gaps E_{bnd} of the inner shells by setting $\text{Im}\epsilon(k,\omega) = 0$ if $|\hbar\omega| < E_{\text{bnd}}$ with consistent adaptation of $\text{Re}\epsilon$ by a Kramers-Kronig analysis. Results from inserting orbital binding energies of isolated atoms[7,24] into E_{bnd} show that this suppression of the inner target shell contributions removes the 5–10 % surplus of the Kaneko proton cross sections compared to the ZBL database. Though this variant takes even more influence on the heavy-ion cross sections, we shall present results obtained from the original model. At low v the changes cancel partially, at high v massively, if we build the ratio of cross sections and γ, which we concentrate on.

B. Effective charge and Fermi velocity

The ZBL calculations basically derive heavy-ion stoppings by insertion of formula (8) into (1). That means that the dependence of the cross section on individual targets is mainly brought in by the experimental proton stopping data, whereas the effective-charge fractions are only controlled by the free and valence target electrons in terms of the Fermi velocity.

The Kaneko model supports this simplifying replacement of $\gamma(Z_2)$ by a $\gamma(v_F)$: Squared effective-charge fractions from the Kaneko theory for protons and heavy ions are given in Fig. 9. The stopping numbers L were numerically integrated shell by shell, using (7). Sometimes two different q values have been chosen to check that our qualitative observations are independent of the ionization fraction. The effective-charge fraction γ is predicted to be a rising function of the target Fermi velocity [Fig. 9(b)]. This statistical point of view legitimizes the simplified ansatz $\gamma(v_F)$. The comparison is consciously done with the Fermi velocities tabulated by ZBL, not with values derived from the number of free electrons in the Kaneko theory. The range of validity of (8) is not overestimated this way. The reason for this correlation between γ and v_F is made clear in Fig. 10: The target shells of localized electrons build a much higher percentage of the total cross section of the heavy ion than of the proton at small v. Therefore, the cross section $S(Z_2)$ is rather smooth in the case of the heavy ion, but anticorrelated with v_F in the case of the proton. Their quotient and eventually γ in our mixed BK-Kaneko theory must be positively correlated with v_F.

The formula of the L integral lets us also understand why heavy ions with small q owe a larger part of their total cross sections to the bound target electrons than the pointlike protons. The heavy-ion form factor $\rho_m(z)$ suppresses the low-z contributions from the u integral, whereas the constant factor of the proton collects all alike. At the same time, for loosely bound or free target electrons the maximum of the u integral, the energy loss function, is localized at smaller z. Building the product and integrating over scaled wave numbers z means that the heavy ion looks screened for small z (small momentum exchange), where the free electrons dominate the target excitation spectrum. It looks like the full core charge for large z, where the inner target shells may be excited.

Kaneko's $\gamma(Z_2)$ of fixed ionization fractions [Fig. 9(a)] is a much more varying function than the nearly flat ZBL results at small and medium velocities. First, this may be attributed to known imperfections of the BK ion model at low velocities, e.g., the absence of Z_1 oscillations, as discussed in Sec. III A. Second, a simultaneous dependence of q on v_F, which must be stronger than used in the ZBL program, would be able to reduce the residual γ oscillations.

A slight rise of $\gamma(Z_2)$ at large ion energies is predicted, which is correlated with the mean density of all target electrons, not only the subset that is represented by the Fermi velocity [Fig. 9(a)]. This indicates the attainment of a binary encounter level; the ion interacts with target electrons separately, and the cross section per target atom becomes proportional to the total number of electrons per target atom. γ becomes a function of the mean density of *all* target electrons at the ion place in the model. It generalizes the interpretation by BK (Ref. 2) for free-electron targets that $\gamma - q$ quantifies the point character of the ion by comparing its size parameter with the target-electron distance. The ZBL effective charges, however, do not depend on Z_2 at large ion velocities. The nonconformity may suggest that, for example, the models of effective-charge theory are wrong in placing the ion *on* but should place it *in* the target electrons, pushing them away. Furthermore, the deviation of the ion path from a straight line trajectory during the ion-atom collisions may introduce a different effective statistical weight of the target shell contributions.

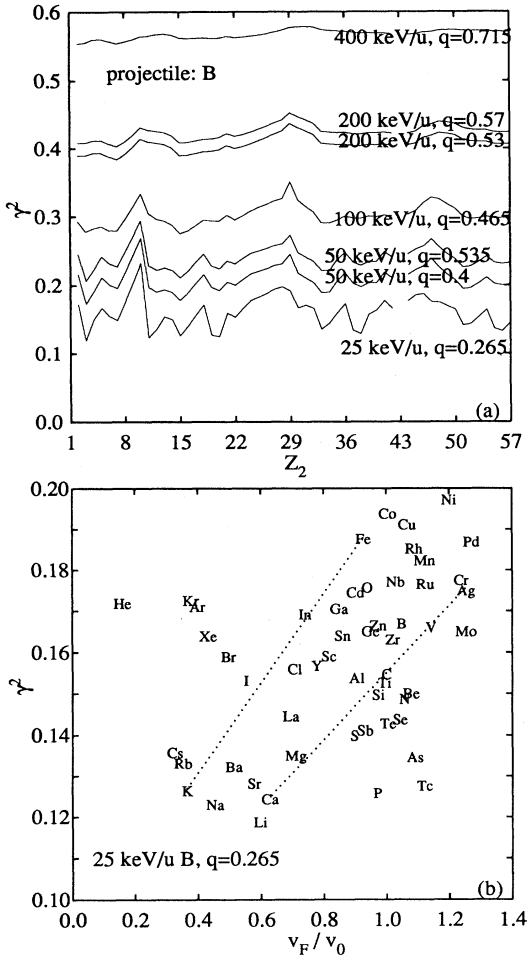

FIG. 9. (a) Squares of effective-charge fractions from the Kaneko target model (solid-state parameters), the BK ion model, and constant ionization fractions. (b) One of these sets versus the ZBL target Fermi velocity instead of the atomic number. Targets — like solid rare gases or $_{43}$Tc — that have likely had little experimental significance and statistical weight in the ZBL data basis should be left aside when drawing conclusions from the figure. The dashed lines only serve as a guide to the eyes.

C. Effective-charge fractions by free-electron subshells

Complementary to the previous section, the Kaneko theory allows for another kind of test whether a restriction to the subset of the free target electrons is possible.

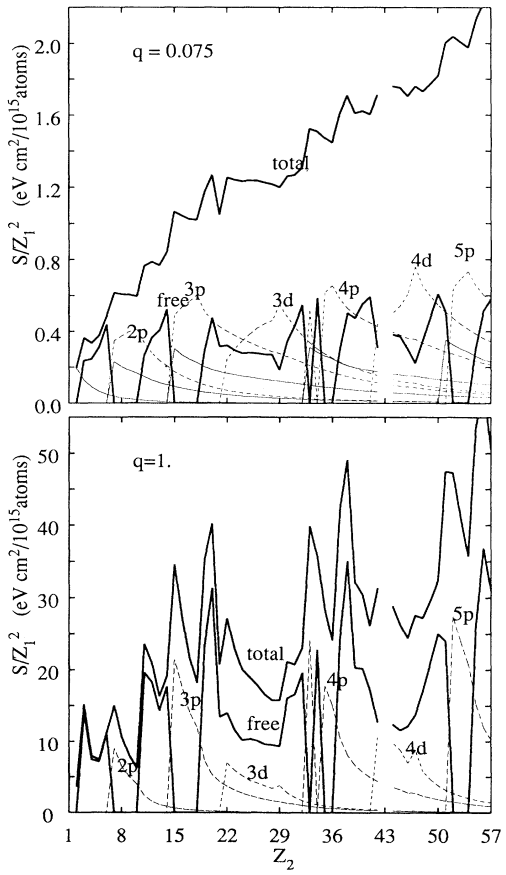

FIG. 10. Individual shell contributions to the total stopping from the Kaneko theory for $Z_1 = 15$ (top figure) and protons (bottom figure) with $v = v_0$ and BK form factor. Upper thick lines denote total cross sections S, lower thick lines shares of free electrons $N_{\text{free}}S_{\text{free}}$, thin lines of selected s, p, and d shells, $N_{\text{bnd}}S_{\text{bnd}}$.

This time we keep the target fixed and choose the ion velocity as the variable. Within the Kaneko theory the squared effective-charge fractions

$$\gamma^2 = \frac{S(Z_1, q, v)}{Z_1^2 S(Z_1 = 1, q = 1, v)} \tag{15}$$

are compared with the corresponding ratios of the subset of free electrons:

$$\frac{S_{\text{free}}(Z_1, q, v)}{Z_1^2 S_{\text{free}}(Z_1 = 1, q = 1, v)}. \tag{16}$$

For a quantitative test, heavy-ion ionization fractions q must be provided first. For example, insertion of the ZBL ionization fractions into the mixed BK-Kaneko model leads to heavy-ion stoppings that exceed the ZBL values more and more if Z_1 increases. Therefore we varied q in the BK charge model, until the Kaneko theory reproduces the ZBL effective-charge fraction. The resultant values of (15) and (16) are compared in Fig. 11.

The approximative replacement of the "full target" ratio by the "free-electron subshell" ratio works well for high ion velocities and sometimes, including the semiconductor targets $_{14}$Si and $_{32}$Ge, down to medium velocities. Though in our examples the free-electron subshell never contributes more than 40% to the total stopping cross sections at high velocities, a strong and precise cancellation of the remaining subshells may equalize (15) and (16). The necessary condition is that the free electrons give the same percental contribution to the heavy-ion and proton stopping powers, but not that this percentage is large. This condition is automatically fulfilled in the Bethe limit of binary ion-electron collisions (cf. Sec. IV B), when the free target electrons share the ratio $N_{\text{free}}/(N_{\text{free}} + \sum N_{\text{bnd}})$ of the stopping power of any projectile, heavy ions or protons.

That means, although the direct calculation of heavy-ion or proton stopping powers using the free-electron target model and the electron density taken from experimental Fermi velocities is highly inaccurate, their ratio yields reasonable effective-charge fractions.

At least two factors are recognized that validate this scaling even at low velocities: first, if the ion has small Z_1 and is therefore highly stripped or pointlike even at small v. Second, the "free-electron approximation" works better, if more of the target electrons are assumed to be free, better for the semiconductors Si and Ge (4 of 14 and 32) than the metals Ni and Fe (2 of 28 and 26). The nonequivalence of the number of free electrons in the Kaneko theory to the experimental Fermi velocities v_F used by ZBL introduces some arbitrariness of the comparisons. For Si, $v_F = 0.974 v_0$ corresponds to 4.2 electrons evenly distributed in the crystal; for Ni, $v_F = 1.2 v_0$ corresponds to 4.3 electrons; i.e., the cross section of about two d electrons should be added to the two free electrons before building the fraction (16). The example of the Fe target has been added to show that this nonequivalence need not be responsible for the worse agreement of the Ni ratios: The Fe value $v_F = 0.927 v_0$ corresponds to 2.1 electrons evenly distributed in the crystal in good accordance with Kaneko's partitioning, but does not give better agreement of the ratios.

The mismatch of the curves at $v \lesssim 2v_0$ is rather caused by a breakdown of the mixed BK-Kaneko model. For heavy ions at low velocities we can no longer find values of q to fit the small effective charges of ZBL. The model sets lower bounds to the effective charge fractions that are reached by slightly negative q; they increase again if q is chosen more negative. In the example of P on Ni in Fig. 11, negative values of the fitted q had to be used at $v < 2v_0$ to adapt γ to the ZBL values.

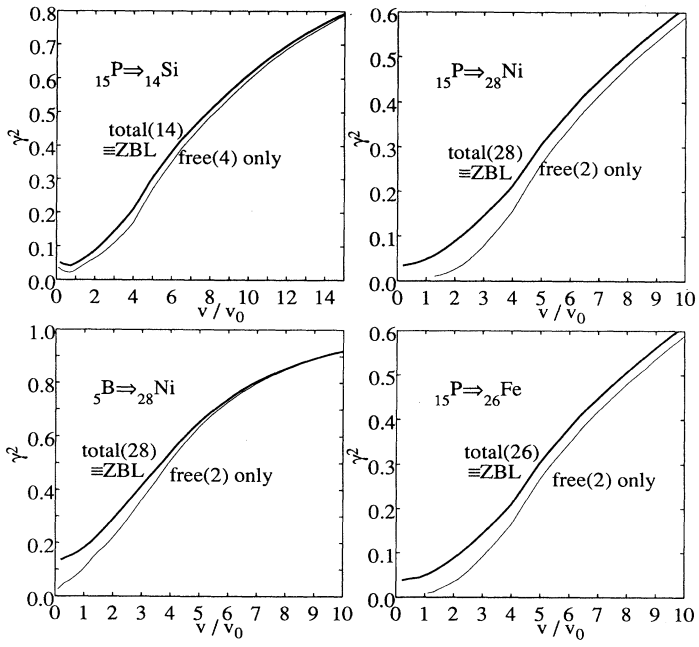

FIG. 11. Comparison of squared effective-charge fractions of the Kaneko theory using the BK form factor. Thick lines: by ratio of the total cross sections, made identical with ZBL by fitting q. Thin lines: by ratio of the cross sections of the free-electron parts only. Numbers in braces are the total number of electrons or number of free electrons per target atom.

V. SUMMARY

Effective-charge theory neatly separates the ion and target properties. It provides much physical insight and is not restricted to ranges of ion atomic numbers or velocities.

There has hitherto been no successful parameter-free explanation of the experimental ionization fractions of medium and heavy ions. The energy criterion is more universal and fundamental than the familiar velocity criterion. Accordance with experiments can be achieved if it is improved by looking at the effectively available energy transfer of target electrons to the ion.

In general, the free-electron gas model of target electrons is highly inaccurate due to the contributions of target inner shell excitations to the charges induced by protons or ions. The inspection by the extended target model of Kaneko verifies that the effective-charge fraction may be interpreted as being built only by the electrons in the top valence or conduction bands. Effective-charge theory may therefore use the effective-charge fraction parametrized by the target Fermi velocity in the heavy-ion scaling rule.

ACKNOWLEDGMENT

This work was supported by the Bundesminister für Forschung und Technologie under Grant No. 211-5291-03-HE3ROS.

[1] J. Lindhard and A. Winther, K. Dan. Vidensk Selsk. Mat. Fys. Medd. **34**, 1 (1964).
[2] W. Brandt and M. Kitagawa, Phys. Rev. B **25**, 5631 (1982).
[3] J. F. Ziegler, J. P. Biersack, and U. Littmark, *The Stopping and Range of Ions in Solids* (Pergamon, New York, 1985), Vol. 1.
[4] A. Mann and W. Brandt, Phys. Rev. B **24**, 4999 (1981).
[5] J. F. Ziegler and J. M. Manoyan, Nucl. Instrum. Methods B **35**, 215 (1988); J. P. Biersack, *ibid.* **80/81**, 12 (1993).
[6] L. Spruch, Rev. Mod. Phys. **63**, 151 (1991).
[7] E. Clementi and C. Roetti, At. Data Nucl. Data Tables **14**, 177 (1974).
[8] T. L. Ferrell and R. H. Ritchie, Phys. Rev. B **16**, 115 (1977).
[9] J. F. Ziegler, in *Handbook of Ion Implantation*, edited by J. F. Ziegler (North-Holland, Amsterdam, 1992), p. 1.
[10] S. Kreussler, C. Varelas, and W. Brandt, Phys. Rev. B **23**, 82 (1981).
[11] P. M. Echenique, R. M. Nieminen, J. C. Ashley, and R. H. Ritchie, Phys. Rev. A **33**, 897 (1986); P. M. Echenique, Nucl. Instrum. Methods B **27**, 256 (1987).
[12] Y. Xia, C. Tan, X. Hu, and L. Mei, Nucl. Instrum. Methods B **82**, 513 (1993); Y. Xia, C. Tan, and W. N. Lennard, *ibid.* **90**, 41 (1994); **90**, 88 (1994).
[13] V. H. Kumar and A. P. Pathak, J. Phys. Condens. Matter **5**, 3163 (1993).
[14] F. Guinea, F. Flores, and P. M. Echenique, Phys. Rev. B **25**, 6109 (1982).
[15] B. S. Yarlagadda, J. E. Robinson, and W. Brandt, Phys. Rev. B **17**, 3473 (1978).
[16] N. Bohr, Phys. Rev. **59**, 270 (1941).
[17] W. Brandt, in *Atomic Collisions in Solids*, Proceedings of the 5th International Conference on Atomic Collisions in Solids, Gatlinburg, Tennessee, 1973, edited by S. Datz, B. R. Appleton, C. D. Moak (Plenum, New York, 1975), Vol. 1, p. 261.
[18] W. E. Lamb, Phys. Rev. **38**, 696 (1940).
[19] L. C. Northcliffe, Phys. Rev. **120**, 1744 (1960).
[20] J. Knipp and E. Teller, Phys. Rev. **59**, 659 (1941).
[21] M. J. Puska, R. M. Nieminen, and M. Manninen, Phys. Rev. B **24**, 3037 (1981).
[22] T. Kaneko, Phys. Status Solidi B **156**, 49 (1989); At. Data Nucl. Data Tables **53**, 272 (1993).
[23] T. Kaneko, Surf. Sci. **236**, 203 (1990).
[24] A. D. McLean and R. S. McLean, At. Data Nucl. Data Tables **26**, 197 (1981).